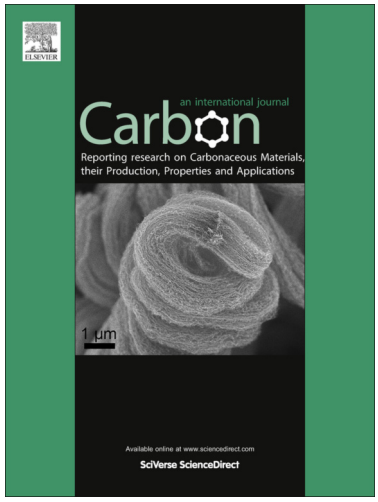

A hydrothermal route to water-stable luminescent carbon dots as nanosensors for pH and temperature

Chuanxi Wang, Zhenzhu Xu, Hao Cheng, Huihui Lin, Mark G. Humphrey, Chi Zhang

PII: S0008-6223(14)00997-X
DOI: http://dx.doi.org/10.1016/j.carbon.2014.10.035
Reference: CARBON 9428

To appear in: *Carbon*

Received Date: 25 July 2014
Accepted Date: 14 October 2014

Please cite this article as: Wang, C., Xu, Z., Cheng, H., Lin, H., Humphrey, M.G., Zhang, C., A hydrothermal route to water-stable luminescent carbon dots as nanosensors for pH and temperature, *Carbon* (2014), doi: http://dx.doi.org/10.1016/j.carbon.2014.10.035

A facile hydrothermal route to prepare water-stable luminescence carbon dots as nanosensor for pH and temperature

Chuanxi Wang,*[a] Zhenzhu Xu,[a] Hao Cheng,[a] Huihui Lin,[a] Mark G. Humphrey[b] and Chi Zhang*[a]

[a]*China-Australia Joint Research Centre for Functional Molecular Materials, School of Chemical & Material Engineering, Jiangnan University, Wuxi 214122, P. R. China*

[b]*Research School of Chemistry, Australian National University, Canberra, ACT 0200, Australia*

Corresponding author. E–mail address: chizhang@jiangnan.edu.cn (C. Zhang); wangcx@jiangnan.edu.cn (C. Wang)

Abstract

Carbon dots (CDs) as a class of heavy-metal-free fluorescent nanomaterials has drawn increasing attention in recent years due to their high optical absorptivity, chemical stability, biocompatibility, and low toxicity. Herein, we report a facile method to prepare stable CDs by hydrothermal treatment of glucose (glc) in the presence of glutathione (GSH). With this approach, the formation and the surface passivation of CDs are carried out simultaneously, resulting in intrinsic fluorescence emission. The influence of reaction temperature, reaction time and feed ratio of GSH/glc on the photoluminescence property of CDs is studied. The as-prepared CDs are characterized by UV–Vis, photoluminescence, X–ray photoelectron spectroscopy, Fourier transform infrared spectroscopy and transmission electron microscope, from which their structural information and property are interpreted. Owning to their pronounced temperature dependence of the steady-state fluorescence emission spectra and pH-responsive behavior, resultant CDs could work as versatile nanothermometry devices by taking advantage of the temperature sensitivity of their emission intensity, which change considerably over the physiological temperature range (15–60 ºC), as well as a sensor for pH.

1. Introduction

Temperature and pH are fundamental thermodynamic variables which strongly affect biochemical and physiological actions and/or processes [1]. The accurate measurement of them is of increasing importance due to their widespread applications (electronic devices, biology, medical diagnostics) [2]. Up to now, some promising materials to local temperature/pH sensing are being designed, including scanning probe microscopy, Raman spectroscopy, and fluorescence-based measurements [3–5]. Among them, fluorescence-based nano-sensors are of particular interest because of their fast response, high spatial resolution, and safety of remote handling [6]. Indeed, several fluorescent nanomaterials, using semiconductor quantum dots (QDs), organic dyes, fluorescent polymers have been reported for temperature detection, which operates by the temperature-dependant luminescence intensity and/or decay time [7–9]. Moreover, fluorescent metal nanoclusters have already shown great potential for temperature/pH sensor in water or in biological systems, and especially live cells [10, 11]. However, the drawbacks of these existing methods are low sensitivity, systematic errors due to fluctuations in the fluorescence rate, the toxicity and the stability of optical properties in the local chemical environment/surrounding medium, which limits their further applications. Recently, fluorescent carbon dots (CDs) have been applied in ratiometric pH sensing in cells [12], while few CDs thermometers is reported.

The development of heavy-metal-free fluorescent nanomaterials as novel probes has drawn increasing attention in recent years [13–15]. Carbon nanopartciles or CDs as a class of heavy-metal-free fluorescent nanomaterials possess some advantageous, such as tunable emission, high optical absorptivity, chemical stability, biocompatibility, and low toxicity [16–19]. These superior properties make them promising candidates for numerous exciting applications, for example in bioimaging, biosensor, catalysis and photovoltaic devices [20–23]. Indeed, fluorescent CDs with a diameter less than 10 nm could be prepared produced from bulk graphite materials, candle soot, active carbon, pyrolysized polymers or carbohydrates through various methods (laser irradiation, electrochemical oxidation, microwave treatment,

hydrothermal treatment or strong acid oxidation) [24–28]. Hydrothermal is a facile and effective synthesis approach to produce fluorescent CDs from citric acid [29], glucose [30] and orange peels [31]. On the other hand, the stability of fluorescent nanomaterials is an important factor for their applications, and this characteristic heavily depended on the chemical nature of the surface ligands and the interface between the core and the organic ligands [32]. To achieve a robust stability of fluorescent nanomaterials, the most direct and valid method is using capping molecules to form strong chemical bonds linking to the surface atoms of the core [33]. Although a large number of researches focus on the preparation of water-soluble luminescence CDs, the instability makes them unsuitable for using in the local chemical environment.

Glutathione (GSH), a naturally occurring and readily available tripeptide, is usually used as template and protecting in synthesizing fluorescent nanomaterials [34]. Moreover, many functional groups of GSH, including thiols, carboxyl and amino groups make fluorescent nanomaterials exhibit good dispersion and photo-stability in aqueous solution [35]. For example, Lin group reported fluorescent gold nanodots with GSH as protecting layer and resultant gold nanodots showed excellent photoluminescence properties with high photo-, time-, metal-, and pH-stability [36]. Herein, a facile hydrothermal route is designed to prepare luminescence CDs using glucose as C source. As-prepared CDs emit blue luminescence and passivity with GSH which makes them exhibit excellent water-soluble and -stable properties. More importantly, resultant blue luminescence CDs could be used as nanoprobes for temperature and pH sensing in liquids.

2. Experimental

2.1 Materials

Glucose (glc), quinine sulfate and reduced glutathione (GSH) are purchased from Aldrich and used as received without further purification. All the salts (analytical reagent) are obtained from Sinopharm Chemical Reagent Co., Ltd and used without further purification. The solutions of 20 mM of NaCl, KNO_3, NH_4Cl, $ZnCl_2$, $Ba(NO_3)_2$, $FeCl_2$, $Ca(NO_3)_2$, $MgSO_4$, $Cu(NO_3)_2$, $Ni(NO_3)_2$, $(CH_3COO)_2Mn$, $Co(NO_3)_2$,

$Cd(NO_3)_2$, $PbCl_2$, $(CH_3COO)_3Cr$ are prepared, respectively. De–ionized water is used in all experiments.

2.2 Preparation of intensively fluorescent carbon dots

0.02 g of glc and 0.1 g of GSH with the molar ratio of glc/GSH of 1/3.5 are dissolved in 10 mL of deionized water in a glass beaker. After stirring for 3 min, the mixture is transferred to a Teflon-lined autoclave chamber. After that, the chamber is sealed and put into an oven. Upon completion of hydrothermal reaction in the oven at 180 ºC for 22 hours, the reaction product is centrifuged at 8500 rpm for 15 minutes to remove the black precipitates after cooling to room temperature. The yellow supernatant is collected and filtered through a PTFE syringe filter with pore size of 0.22 μm. Then the solution is subjected to dialysis in order to obtained high quality carbon dots (CDs). Resultant CDs are stored in the dark for future using.

2.3 Quantum Yield Calculations

The quantum yield (QY) of the CDs is found by comparing the integrated photoluminescence (PL) intensities (excited at 350 nm) and the absorbance values (at 350 nm) of the CDs using quinine sulfate as a reference. In order to minimize re-absorption effects, absorption in the 10 mm fluorescence cuvette is kept below 0.10 at 350 nm excitation wavelength. Quinine sulfate with QY=0.54 is dissolved in 0.1 M H_2SO_4 (refractive index of 1.33) while the CDs are dissolved in water (refractive index of 1.33). A RF-5301PC spectrophotometer set with an excitation slit width of 0.3 nm and an emission slit width of 0.3 nm is used to excite the samples at 350 nm and to record their PL spectra. The integrated PL intensity is the area under the PL curve in the wavelength range from 370 to 600 nm.

The QY was calculated using the below equation:

$$\Phi_X = \Phi_{ST}(I_X/I_{ST})\ (A_{ST}/A_X)(\eta_X^2/\eta_{ST}^2)$$

Where Φ is the QY, I is the measured integrated PL intensity, η is the refractive index of the solvent, and A is the optical density. The subscript "ST" refers to standard with known QY and "X" for the sample.

2.4 Adjusting the pH of aqueous solution of the obtained carbon dots

HCl (2 M) or NaOH (2 M) is used to adjust the pH of the aqueous solution of resultant CDs.

2.5 Ion stability of the obtained carbon dots

To investigate whether this system is stable for some common ions, the effects of 15 other kinds of cations, including Na^+, K^+, NH_4^+, Zn^{2+}, Ba^{2+}, Fe^{2+}, Ca^{2+}, Mg^{2+}, Cu^{2+}, Ni^{2+}, Mn^{2+}, Co^{2+}, Cd^{2+}, Pb^{2+}, and Cr^{3+}, on the fluorescence response of as-prepared CDs are recorded by fluorescence spectrophotometer. Briefly, 1.0 ml of solutions of NaCl, KNO_3, NH_4Cl, $ZnCl_2$, $Ba(NO_3)_2$, $FeCl_2$, $Ca(NO_3)_2$, $MgSO_4$, $Cu(NO_3)_2$, $Ni(NO_3)_2$, $(CH_3COO)_2Mn$, $Co(NO_3)_2$, $Cd(NO_3)_2$, $PbCl_2$, and $(CH_3COO)_3Cr$ with the concentration of 20 mM are added into 1.0 ml of the as-prepared CDs. The mixture is stirred for 3 min and then the fluorescence spectra of the mixture are investigated under the optimum conditions.

2.6 Characterization Methods

UV–Vis absorption spectrum is obtained by using a TU–1991 UV–Vis spectrophotometer. Photoluminescence (PL) experiments are performed with a Shimadzu RF–5301 spectrofluorimeter. X–ray photoelectron spectroscopy (XPS) using Mg K_α excitation (1253.6 eV) is collected in a VG ESCALAB MKII spectrometer. Binding energy calibration is based on C 1s at 284.6 eV. The Fourier transform infrared spectroscopy (FTIR) is measured at wavenumbers ranging from 500 cm^{-1} to 4000 cm^{-1} using a Nicolet 6700 FTIR spectrophotometer. The morphology and mean diameter of resultant CDs are characterized by JEM–2100 transmission electron microscope (TEM) operating at 200 kV.

3. Results and Discussion

3.1 Synthesis of fluorescent carbon dots

The procedure of preparing strongly fluorescent and highly stable carbon dots (CDs) is simple as shown in Fig. 1. The synthetic approach follows the controlling hydrothermal treatment (180 ºC) of glucose (glc) in the presence of glutathione (GSH) for 22 h. With this approach, the formation and the surface passivation of CDs are carried out simultaneously, resulting in intrinsic fluorescence emission. Although the origins of photoluminescence (PL) are not yet entirely understood in CDs, there is

mounting evidence that emission arises from the radiative recombination of excitons located at surface energy traps which may or may not require passivation by organic molecules to occur [37]. Surface passivation could produce defect sites on the surface of CDs and the fluorescence emission arises from the radiative recombination of the excitons trapped by the defects [38]. We consider that the formation of CDs and their surface passivation take place simultaneously during hydrothermal treatment of glc in the presence of GSH. The abundant functional groups, such as carboxyl acids and amines identified by X–ray photoelectron spectroscopy (XPS) and Fourier transform infrared spectroscopy (FTIR) spectra, can introduce different defects on the surface, acting as the excitation energy traps and leading to the different PL properties.

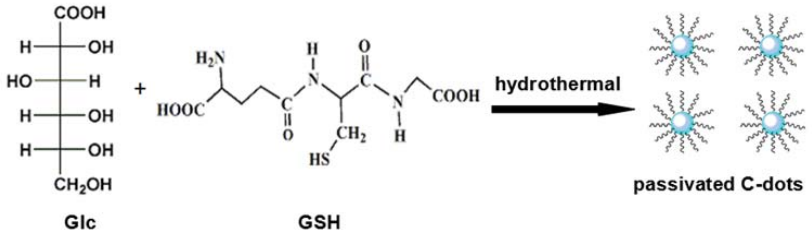

Fig. 1-One-step route to synthesize surface passivated CDs by hydrothermal treatment of glc in the presence of GSH.

To find the optimal reaction conditions, we investigate the fluorescence spectra of resultant CDs under different molar ratio of GSH and glc, reaction temperature and reaction time (Fig. S1). By changing the weight ratio in the process of reaction, we obtain fluorescence spectra of resultant CDs under different molar ratio of GSH and glc. As shown in Fig. S1a, the emission spectra of CDs with molar ratios of 1:1, 2:1, 4:1 and 5:1 of GSH and glc were analogous, so we preliminarily conclude that reactant ratio have no obvious impacts on the fluorescent properties of the resultant CDs in our experiment. Then, the effect of reaction time on the preparation of CDs is investigated. As shown in Fig. S1b, the increase in heat-up time could make the enhancement of fluorescent intensity and narrower the full width at half maximum (FWHM). In addition, comparing with the reaction temperature of 80 and 120 ºC,

fluorescence spectra under reaction temperature of 150 and 180 ºC have obvious red shift and also a narrower FWHM (Fig. S1c).

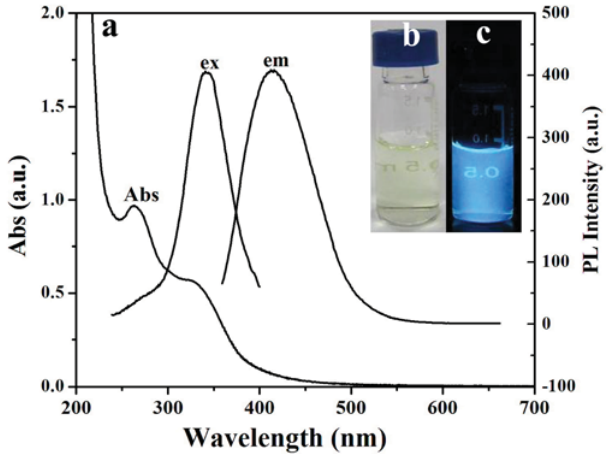

Fig. 2-(a) UV–Vis absorption, (ex) excitation and (em) emission spectra of resultant fluorescent CDs in aqueous solution; the photographs of fluorescent CDs: (b) under room light and (c) under 365 nm UV light illumination. The measurements are performed under room temperature with the pH=3.

Fig. 2 depicts the UV–vis and fluorescence spectra of the diluted solution of resultant CDs in aqueous solution. In the UV–vis spectrum (Fig. 2a), it is seen that there are two UV–vis absorption peaks at 264 and 330 nm, respectively. The peak at 264 nm is typically ascribed to the π-π* transition of aromatic sp2 domains [31, 39]. The peak at 330 nm is attributed to the n-π* transition of C=O band [40]. As shown, an optical absorption peak at 330 nm matches with the maximum fluorescence excitation (ex). In aqueous solution, the CDs exhibit blue fluorescence with λmax at 471 nm and the FWHM around 100 nm (Fig. 2a). The diluted solution of the as-prepared CDs in aqueous solution is nearly colorless (or a very slight yellow color) under visible light (Fig. 2b), while it emits intense blue fluorescence under 365 nm UV light illumination (Fig. 2c). The quantum yield (QY) of the as-prepared CDs in aqueous solution at room temperature is found to be 7.2% using quinine sulfate (0.1M H_2SO_4 as solvent; QY=0.54) as a reference.

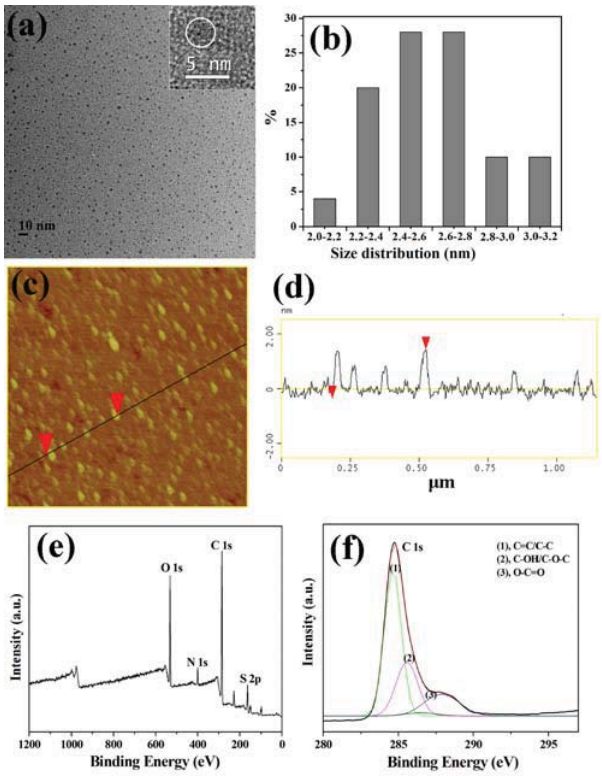

Fig. 3-(a) TEM image of resultant fluorescent CDs; (b) size distribution: the average size was 2.6 ± 0.2 nm; (c) AFM image of resultant fluorescent CDs; (d) the height profile along the line of Fig. 3c; XPS survey (e) and XPS C1s (f) spectra of CDs.

The size and morphology of CDs are characterized using transmission electron microscopy (TEM) and atomic force microscopy (AFM) (Figs. 3a and 3c). The TEM images reveal that the CDs particles are spherical with an average diameter of 2.6 ± 0.2 nm (Fig. 3b). In addition, none of lattice fringes is observed in the corresponding high resolution TEM (HRTEM) image (inset of Fig. 3a), indicating the amorphous nature of the CDs. The AFM image also supports the spherical morphology, with average heights of 1.8 ± 0.2 nm (Fig. 3d). CDs are characterized using XPS in order to explore their elemental composition and chemical bonds. The presence of C, O, N and S in the as-prepared CDs is confirmed by XPS (Fig. 3e). The high resolution XPS spectra of C 1s (Fig. 3f) are divided into three unit moieties: C=C/C−C with a binding energy at 284.5 eV; C−OH/C−O−C at 285.9 eV; and O−C=O at 288.4 eV [31, 41]. On the other hand, the high resolution XPS spectra of N 1s, O 1s and S 2p (Fig. S2) confirm that C–N, C–O, C=O, N–H, S and oxidized sulfur bonds exist in CDs [42].

These results indicate that there are apparent hydrophilic functional groups on the surface of the as-synthesized CDs. These hydrophilic groups can help CDs disperse into aqueous solution. FTIR spectra (Fig. S3) are used to identify the surface functional groups present on the CDs' surface. In the FTIR analysis of CDs, the following are observed: stretching vibrations of O–H and N–H at ~3400 cm^{-1}, C−H at ~2900 cm^{-1}, and =C−H at 3090 cm^{-1}, stretching vibrations of C=O at 1670 cm^{-1}, bending vibrations of N–H at 1570 cm^{-1}, and the vibrational absorption band of C−N at 1180 cm^{-1} and 1030 cm^{-1} [43]. The results from FTIR spectra agree well with the XPS results showing that there are hydrophilic functional groups on the surface of the as-prepared CDs due to the surface passivation with GSH.

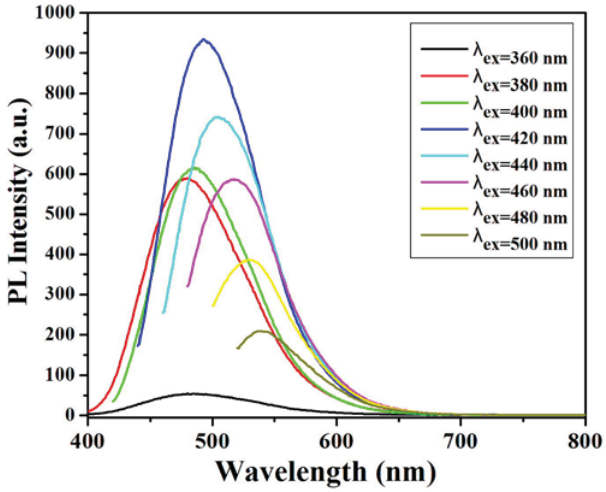

Fig. 4-PL emission spectra of the surface passivated CDs in water obtained by excitation wavelengths from 360 to 500 nm. The measurements are performed under room temperature with the pH=3

Excitation-dependent PL behavior is observed, which is common for fluorescent carbon materials [44]. Fortunately, excitation-dependent PL behavior can be useful in multi-color imaging applications [18, 45]. The emission spectra of the as-synthesized CDs from 478 nm to 545 nm (Fig. 4) show change in the PL intensity as the excitation wavelength varied from 360 nm to 500 nm. CDs achieve the maximum emission intensity around 494 nm (a bright blue emission) when it is excited at 420 nm. The surface state and size effect affecting the band gap of CDs are considered to be reasons for the complexity of the PL behavior [25, 39, 44, 45].

3.2 High Stability of fluorescent carbon dots

The stability of luminescent nanomaterials is an important factor to assess their applications [33, 36]. Herein, as-prepared CDs are exposed under a 450 W xenon (Xe) lamp for various time spans to probe their photo-stability. The fluorescence intensity of as-prepared CDs decrease only slightly, and preserve ~92% of the initial intensity even after 120 min irradiation by 450 W Xe lamp (Fig. 5a), which has been much more stable than FITC dye or CdTe QDs [33]. The fluorescence spectra of the as-prepared fluorescent CDs irradiated by a 450 W xenon lamp at various time in detail are given in Fig. S4a.

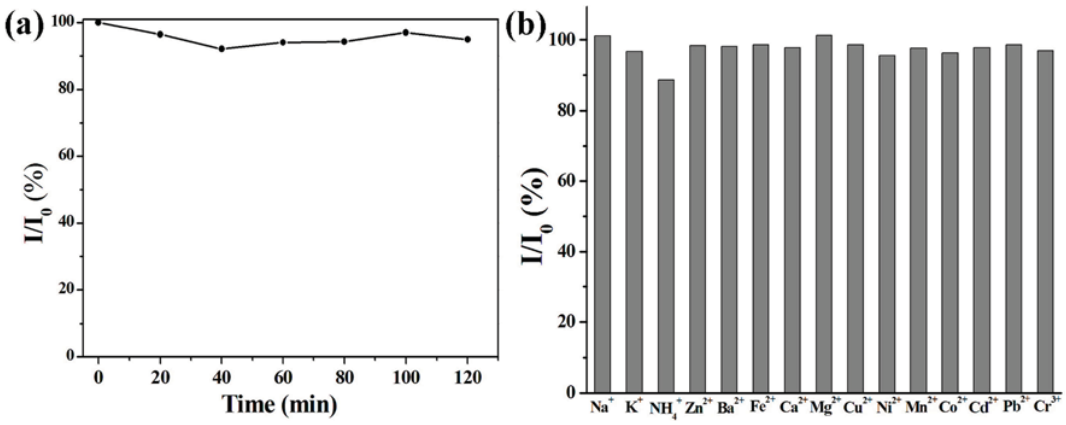

Fig. 5-The fluorescent stability of CDs : (a) Photo stability of as-prepared CDs irradiated by a 450 W xenon lamp at various time and (b) the metal stability of CDs in various metal ions with the concentration of 10^{-2} M.

In addition to the photo-stability, ions-stability is another factor that we cannot ignore in ensuring fluorescent nanomaterials to achieve practical applications [10]. The stability is investigated by the interference of some common cations (0.01 M) with the as-prepared fluorescent CDs. The relative fluorescence intensity is determined by calculating the ratio of the fluorescence intensities of CDs solution in the presence and absence of the interference ions as shown in Fig. 5b. The results revealed that most of these ions show either no or slight interference proving that these common cations did not play a part in impairing the fluorescence intensity of the as-prepared CDs. The fluorescence spectra of the as-prepared CDs in some common

cations (0.01 M) in detail are given in Fig. S4b. Moreover, there is no obvious change in the fluorescence intensity for as-prepared CDs after storing for one month under normal condition (Fig. S5). In a word, the as-prepared CDs with good photo-, time- and ions-stability in this article are particular appropriate for practical applications. We argue the high stability of the resultant CDs caused by surface passivation of GSH. GSH, an abundant triamino acid peptide in nature, containing free thiol, carboxyl and amine groups which have been confirmed by XPS and FTIR results, could form a protective shell around the CDs [48].

3.3 Optical responses of fluorescent carbon dots to pH

When the stability of the fluorescent CDs at different pH values is assessed, surprisingly strong optical responses to changes in pH are observed. A series of fluorescent CDs solutions with pH ranging systematically from 1 to 13.5 are prepared, and the fluorescence intensity of fluorescent CDs in different pH values is monitored with a spectrofluorimeter. Significant changes in emission intensity are observed as the pH is varied, as depicted in Fig. 6a. It is obvious that the emission intensity reaches the maximum value at pH=3 but it decreases dramatically from pH=3 to pH=10 and changes a little at higher pH values (10–13). Meanwhile, a blue-shift in the emission peak from 487 to 472 nm is observed as pH decreases from 4 to 1 (Fig. S6a).

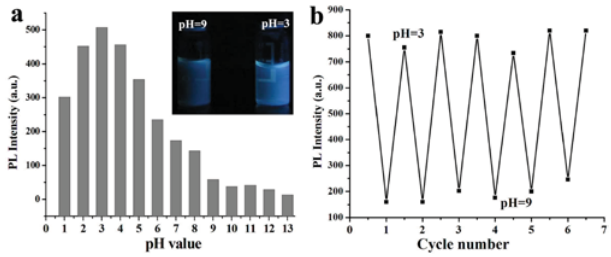

Fig. 6-(a) PL intensity of CDs at various pH values; (b) PL intensity upon the cyclic switching of CDs under alternating conditions of pH=3 and pH=9.

To evaluate the reversibility of the switching operation upon variation of pH, the as-prepared CDs are subjected to pH cycling between pH=3 and pH=9 using acid and base as modulators. As shown in Fig. 6b, the luminescence switching operation can be

repeated for six consecutive cycles without fatigue, indicative of good reversibility of the two-way switching processes. The fluorescence spectra of the as-prepared fluorescent CDs upon the cyclic switching of CDs under pH=3 and pH=9 in detail are given in Fig. S6b.

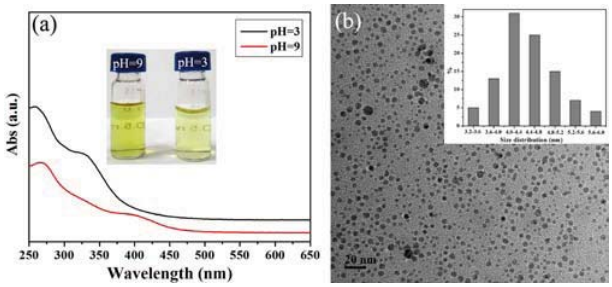

Fig. 7-(a) UV–Vis absorption spectra of CDs in aqueous solution under pH=3 and pH=9, inset display the photographs of CDs under room light at pH=3 and pH=9; (b) the TEM image of CDs in aqueous solution at pH=9 and the size increases up to 4.6 ± 0.2 nm.

To gain more insight into the origin of the PL behavior, and explain strong optical responses to changes in pH of CDs, TEM and UV–vis spectra are performed. As shown in Fig. 7a, the as-prepared CDs display a obvious change in the UV–Vis spectra upon increasing the pH value from pH=3 to pH=9. In the aqueous solution with high pH value of 9.0, the absorption peak at 405 nm exhibits an obvious red-shift by comparison with the CDs of pH=3. Upon raising the pH value, CDs are transformed to a electronegative form resulting in red shift of the absorption peak due to the electronic effect of the surface groups, which is correspond to the fluorescence spectra (Fig. S6). We attribute the observed red shift of the absorption peak to both of the formation of larger particles and the incensement of pH value. It is found that the average diameter of CDs under pH=9 is 4.6 ± 0.2 nm (Fig. 7b), while the average diameter of CDs under pH=3 is 2.6 ± 0.2 nm (Fig. 3a). Obviously, the increase in diameter of CDs between pH=3 and pH=9 is detected. Correspondingly, the color of the solutions changed from light yellow to dark yellow as the pH value increased from 3 to 9 (the set of Fig. 7a). The results confirmed that under low pH values, the CDs were dissolved as isolated species in the aqueous; in contrary, the aggregation CDs

appeared with increasing the pH value because of noncovalent molecular interactions, such as hydrogen bonds between the carboxyl groups [49]. Hence, pH-induced aggregations of the as-prepared CDs result in an obvious fluorescence quenching at high pH values.

3.4 Optical responses of fluorescent carbon dots to temperature

Fig. 8a shows the pronounced temperature dependence of emission spectra of the as-prepared CDs. The intensity decreases by 52% upon raising the temperature from 15 to 90 ºC. The emission spectra of the as-prepared CDs do not shift within the investigated temperature window. As shown in Fig. 8b, with increasing the temperature from 15 to 60 ºC, the PL intensity of the as-prepared CDs changes close to linearly. Given this temperature range is larger than the physiological temperature, which suggests as-prepared CDs have promising applications in vivo temperature sensing. Moreover, the thermal response of CDs is reversible upon temperature cycling, and there is slight thermal hysteresis during heating and cooling cycles, as shown for four cycles between 20 and 80 ºC in Fig. S7b.

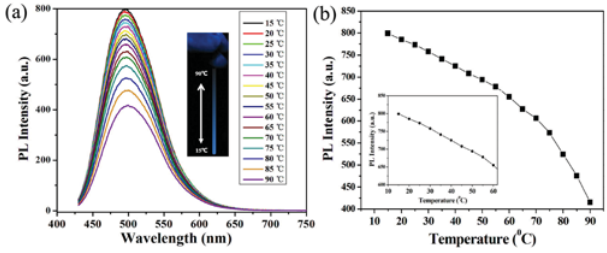

Fig. 8-(a) Fluorescence emission spectra (excitation 400 nm) for various temperatures in the range 15 -90 ºC (top to bottom); (b) the intensity at 500 nm is plotted versus temperature.

Herein, we developed one model to simulate fluorescence change of the various temperatures in the range 15–90 ºC (the set of Fig. 8a). A color change pattern of the temperature gradient is observed. The bottom is strong blue fluorescence and the top is slight blue fluorescence, while the color of the middle part continuously changes from dark blue to light blue as the temperature increases. According to the observation of fluorescence color, the temperature can be readily estimated or measured by

comparison with the temperature-dependent CDs chromaticity diagram. This visualization technique provides a useful tool for the detection of temperature. As illustrated in Fig. 9, TEM and UV–vis spectra are used to study the temperature-responsive PL behavior of CDs. As shown in Fig. 9a, the as-prepared CDs display no change in the UV-vis spectra upon increasing th e temperature from 20 to 80 ºC. It is found that the average diameter of CDs at 80 ºC increased up to 4.4 ± 0.2 nm (Fig. 9b), while the average diameter of CDs at room temperature is 2.6 ± 0.2 nm (Fig. 3a). Hence, increasing the temperature, the aggregation of as-prepared CDs occurred which caused the obvious fluorescence quenching.

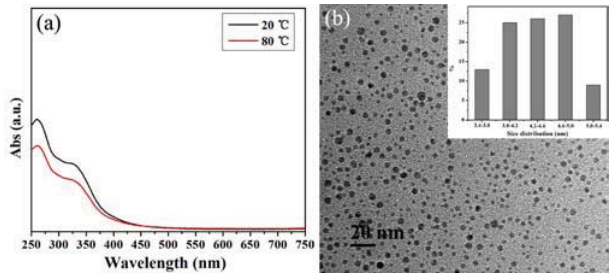

Fig. 9-(a) UV–Vis absorption spectra of CDs in aqueous solution under 20 and 80 ºC; (b) the TEM image of CDs in aqueous solution at 80 ºC and the size increased up to 4.4 ± 0.2 nm.

4. Conclusion

In conclusion, carbon dots (CDs) are prepared by hydrothermal treatment of glucose (glc) in the presence of glutathione (GSH). With this approach, the formation and the surface passivation of CDs are carried out. The chemical structure and PL mechanism are investigated in detail. The as-prepared CDs with good photo-, ions- and time-stability in this article are particular appropriate for practical application. Owning to their pronounced temperature dependence of the fluorescence emission spectra and pH-responsive behavior attribute to temperature-induced and pH-induced aggregation of CDs result in an obvious fluorescence quenching, the obtained CDs have great potential as a novel luminescent thermometer and pH sensor, especially, the photoluminescence intensity is sensitive to temperature and approximately linear in the physiological temperature range which makes the as-prepared CDs be promising candidate in cellular temperature sensing.

Acknowledgements

This work was supported by the National Natural Science Foundation of China (No.50925207), the Natural Science Foundation of Jiangsu Province, China (BK20140157), Programme of Introducing Talents of Discipline to Universities (111 Project B13025), and the Fundamental Research Funds for the Central Universities (JUSRP11418).

Notes and references

[1] Kucsko G, Maurer PC, Yao NY, Kubo M, Noh HJ, Lo PK, et al. Nanometre-scale thermometry in a living cell. Nature 2013;500(7460):54–8.

[2] Okabe K, Inada N, Gota C, Harada Y, Funatsu T, Uchiyama S. Intracellular temperature mapping with a fuorescent polymeric thermometer and fuorescence lifetime imaging microscopy. Nat Commun 2012;3:705–13.

[3] Majumdar A. Scanning thermal microscopy. Annu Rev Mater Sci 1999; 29(1): 505–85.

[4] Kim SH, Noh J, Jeon MK, Kim KW, Lee LP, Woo SI. Micro-raman thermometry for measuring the temperature distribution inside the microchannel of a polymerase chain reaction chip. J Micromech Microeng 2006;16(3):526–32.

[5] Vetrone F, Naccache R, Zamarrón A, Fuente AJ, Francisco SR, Laura MM, et al. Temperature sensing using fluorescent nanothermometers. ACS Nano 2010;4(6):3254–8.

[6] Feng J, Tian KJ, Hu DH, Wang SQ, Li SY, Zeng Y, et al. A triarylboron-based fluorescent thermometer: sensitive over a wide temperature range. Angew Chem Int Ed 2011;50(35):8072–6.

[7] Zhou D, Lin M, Liu X, Li J, Chen ZL, Yao D, et al. Conducting the temperature-dependent conformational change of macrocyclic compounds to the lattice dilation of quantum dots for achieving an ultrasensitive nanothermometer. ACS Nano 2013;7(3):2273–83.

[8] McLaurin EJ, Bradshaw LR, Gamelin DR. Dual-emitting nanoscale temperature sensors. Chem Mater 2013;25(8):1283–92.

[9] Jiang YN, Yang XD, Ma C, Wang CX, Li H, Dong FX, et al. Photoluminescent smart hydrogels with reversible and linear thermoresponses. Small 2010;6(23):2673–7.

[10] Wang C, Wang CX, Xu L, Cheng H, Lin Q, Zhang C. Protein-directed synthesis of pH-responsive red fluorescent copper nanoclusters and their applications in cellular imaging and catalysis. Nanoscale 2014;6(3):1775–81.

[11] Shang L, Stockmar F, Azadfar N, Nienhaus GU. Intracellular thermometry by using fluorescent gold nanoclusters. Angew Chem Int Ed 2013;52(42):11154–7.

[12] Nie H, Li MJ, Li QS, Liang SJ, Tan YY, Sheng L, et al. Carbon dots with continuously tunable full-color emission and their application in ratiometric pH sensing. Chem Mater 2014;26(10):3104–12.

[13] Wu CF, Chiu DT. Highly fluorescent semiconducting polymer dots for biology and medicine. Angew Chem Int Ed 2013;52(11):3086–109.

[14] Peng F, SU YY, Zhong YL, Fan CH, Lee ST, He Y. Silicon nanomaterials platform for bioimaging, biosensing, and cancer therapy. Acc Chem Res 2014;47(2):612–23.

[15] Hola K, Bourlinos AB, Kozak O, Berka K, Siskova KM, et al. Photoluminescence effects of

graphitic core size and surface functional groups in carbon dots: COO^- induced red-shift emission. Carbon 2014;70: 279–86.

[16] Sun YP, Zhou B, Lin Y, Wang W, Fernando KAS, Pathak P, et al. Quantum-sized carbon dots for bright and colorful photoluminescence. J Am Chem Soc 2006;128(24):7756–7.

[17] Fang YX, Guo SJ, Li D, Zhu CZ, Ren W, Dong SJ, et al. Easy synthesis and imaging applications of cross-linked green fluorescent hollow carbon nanoparticles. ACS Nano 2012;6(1):400–9.

[18] Liu RL, Wu DQ, Liu SH, Koynov K, Knoll W, Li Q. An aqueous route to multicolor photoluminescent carbon dots using silica spheres as carriers. Angew Chem Int Ed 2009;121(25):4668–71.

[19] Shen LM, Zhang LP, Chen ML, Chen XW, Wang JH. The production of pH-sensitive photoluminescent carbon nanoparticles by the carbonization of polyethylenimine and their use for bioimaging. Carbon 2013;55:343–9

[20] Ding CQ, Zhu AW, Tian Y. Functional surface engineering of C-dots for fluorescent biosensing and in vivo bioimaging. Acc Chem Res 2014;47(1):20–30.

[21] Yu CM, Li XZ, Zeng F, Zheng FY, Wu SZ. Carbon-dot-based ratiometric fluorescent sensor for detecting hydrogen sulfide in aqueous media and inside live cells. Chem Commun 2013;49(4):403–5.

[22] Yu HJ, Zhao YF, Zhou C, Shang L, Peng Y, Cao YH, et al. Carbon quantum dots/TiO_2 composites for efficient photocatalytic hydrogen evolution. J Mater Chem A 2014;2:3344–50.

[23] Kwon W, Lee G, Do S, Joo T, Rhee SW. Size-controlled soft-template synthesis of carbon nanodots toward versatile photoactive materials. Small 2014;10(3):506–13.

[24] Tao HQ, Yang K, Ma Z, Wan JM, Zhang YJ, Kang ZH, et al. In vivo NIR fluorescence imaging, biodistribution, and toxicology of photoluminescent carbon dots produced from carbon nanotubes and graphite. Small 2012;8(2):281–90.

[25] Wang W, Li YM, Cheng L, Cao ZQ, Liu WG. Water-soluble and phosphorus-containing carbon dots with strong green fluorescence for cell Labeling. J Mater Chem B 2014;2(1):46–8.

[26] Zheng M, Liu S, Li J, Qu D, Zhao HF, Guan XG, et al. Integrating oxaliplatin with highly luminescent carbon dots: an unprecedented theranostic agent for personalized medicine. Adv Mater 2014;26(21):3554–60.

[27] Liu X, H. J. Liu HJ, F. Cheng F, Chen Y. Preparation and characterization of multistimuli-responsive photoluminescent nanocomposites of graphene quantum dots with hyperbranched polyethylenimine derivatives. Nanoscale 2014;6(13):7453–60.

[28] Zhou L, He BZ, Huang JC. Amphibious fluorescent carbon dots: one-step green synthesis and application for light-emitting polymer nanocomposites. Chem Commun 2013;49(73):8078–80.

[29] Zhu SJ, Meng QN, Wang L, Zhang JH, Song YB, Jin H, et al. Highly photoluminescent carbon dots for multicolor patterning, sensors, and bioimaging. Angew Chem Int Ed 2013;52(14):3953–7.

[30] Yang ZC, Wang M, Yong AM, Wong SY, Zhang XH, Tan H, et al. Intrinsicallyfluorescent carbon dots with tunable emission derived from hydrothermal treatment of glucose in the presence of monopotassium Phosphate. Chem. Commun 2011;47(42):11615–7.

[31] Prasannan A, Imae T. One-Pot Synthesis of fluorescent carbon dots from orange waste peels. Ind Eng Chem Res 2013;52(44):15673–8.
[32] Cui Y, Gong XQ, Zhu SJ, Li YH, Su WY, Yang QH, et al. An effective modified method to prepare highly luminescent, highly stable water-soluble quantum dots and its preliminary application in immunoassay. J Mater Chem 2012;22(2):462–9.
[33] He Y, Zhong YL, Peng F, Wei XP, Su YY, Lu YM, et al. One-Pot microwave synthesis of water-dispersible, ultraphoto- and pH-Stable, and highly fluorescent silicon quantum dots. J Am Chem Soc 2011;133(36):14192–5.
[34] Wang CX, Xu L, Wang Y, Zhang D, Shi XD, Dong FX, et al. Fluorescent silver nanoclusters as effective probes for highly selective detection of mercury(II) at parts-per-billion levels. Chem Asian J 2012;7(7):1652–6.
[35] Odriozola I, Loinaz I, Pomposo JA, Grande HJ. Gold-glutathione supramolecular hydrogels. J Mater Chem 2007;17(46):4843–5.
[36] Wang CX, Wang Y, Xu L, Shi XD, Li XW, Xu XW, et al. A galvanic replacement route to prepare strongly fluorescent and highly stable gold nanodots for cellular imaging. Small 2013;9(3):413–20.
[37] Baker SN, Baker GA. Luminescent carbon nanodots: emergent nanolights. Angew Chem Int Ed 2010;49(38):6726–44.
[38] Yang YH, Cui JH, Zheng MT, Hu CF, Tan SZ, Xiao Y, et al. One-step synthesis of amino-functionalized fluorescent carbon nanoparticles by hydrothermal carbonization of chitosan. Chem Commun 2012;48(3):380–2.
[39] Shang JZ, Ma L, Li JW, Ai W, Yu T, Gurzadyan GG. The origin of fluorescence from graphene oxide. Sci Rep 2012;2:792–9.
[40] Chen MY, Wang WZ, Wu XP. One-pot green synthesis of water-soluble carbon nanodots with multicolor photoluminescence from polyethylene glycol. J Mater Chem B 2014;2(25):3937–45.
[41] Bao L, Zhang ZL, Tian ZQ, Zhang L, Liu C, Lin Y,et al. Electrochemical tuning of luminescent carbon nanodots: from preparation to luminescence mechanism. Adv Mater 2011;23(48);5801–6.
[42] Wang CX, Wang Y, Xu L, Zhang D, Liu MX, Li XW, et al. Facile aqueous-phase synthesis of biocompatible and fluorescent Ag_2S nanoclusters for bioimaging: tunable photoluminescence from red to near infrared. Small 2012;8(20):3137–42.
[43] Liu CJ, Zhang P, Tian F, Li WC, Li F, Liu WG. One-step synthesis of surface passivated carbon nanodots by microwave assisted pyrolysis for enhanced multicolor photoluminescence and bioimaging. J Mater Chem 201;21(35):13163–7.
[44] Krysmann MJ, Kelarakis A, Dallas P, Giannelis EP. Formation mechanism of carbogenic nanoparticles with dual photoluminescence emission. J Am Chem Soc 2012;134(2):747–50.
[45] Qu SN, Wang XY, Lu QP, Liu XY, Wang LJ. A biocompatible fluorescent ink based on water-soluble luminescent carbon nanodots. Angew Chem Int Ed 2012;124(49):12381–4.
[46] Zhai XY, Zhang P, Liu CJ, Bai T, Li WC, Dai LM, et al. Highly luminescent carbon nanodots by microwave-assisted pyrolysis. Chem Commun 2012;48(64):7955–7.
[47] Zhu BC, Sun SY, Wang YF, Deng S, Qian GN, Wang M, et al. Preparation of carbon nanodots from single chain polymeric nanoparticles and theoretical investigation of the photoluminescence mechanism. J Mater Chem C 2013;1(3):580–6.

[48] Wang CX, Xu L, Xu XW, Cheng H, Sun HC, Lin Q, et al. Near infrared Ag/Au alloy nanoclusters: tunable photoluminescence and cellular imaging. J Colloid Interf Sci 2014;416:274–9.

[49] Jia XF, Yang X, Li J, Li DY, Wang EK. Stable Cu nanoclusters: from an aggregation-induced emission mechanism to biosensing and catalytic Applications. Chem Commun 2014;50(2):237–9.

TOC

A facile hydrothermal route is designed to prepare water-stable luminescence carbon dots (CDs). As-prepared CDs exhibit blue luminescence and could be used as nanoprobes for temperature and pH sensing in liquids.

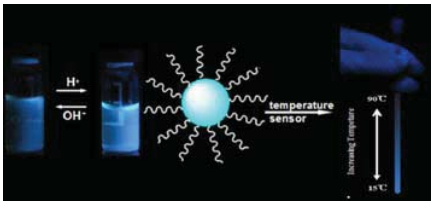

Supplementary Information

A facile hydrothermal route to prepare water-stable luminescence carbon dots as nanosensor for pH and temperature

Chuanxi Wang,*[a] Zhenzhu Xu,[a] Hao Cheng,[a] Huihui Lin,[a] Mark G. Humphrey[b] and Chi Zhang*[a]

[a]China-Australia Joint Research Centre for Functional Molecular Materials, School of Chemical & Material Engineering, Jiangnan University, Wuxi 214122, P. R. China

[b]Research School of Chemistry, Australian National University, Canberra, ACT 0200, Australia

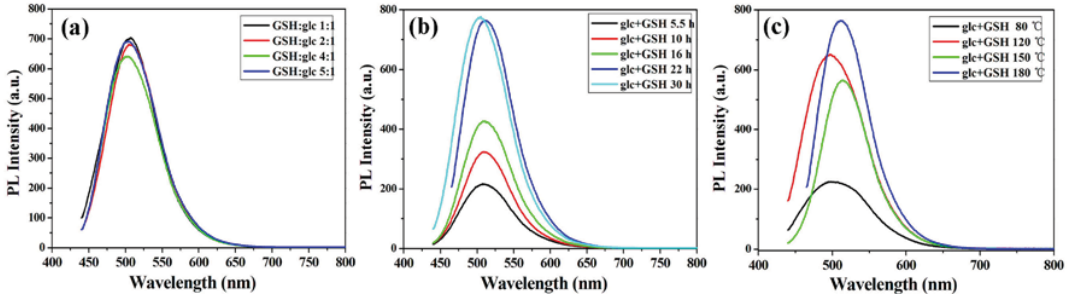

Fig. S1-The fluorescence spectra of resultant CDs under different conditions: (a) molar ratio of GSH and glc; (b) the reaction time; (c) the reaction temperature.

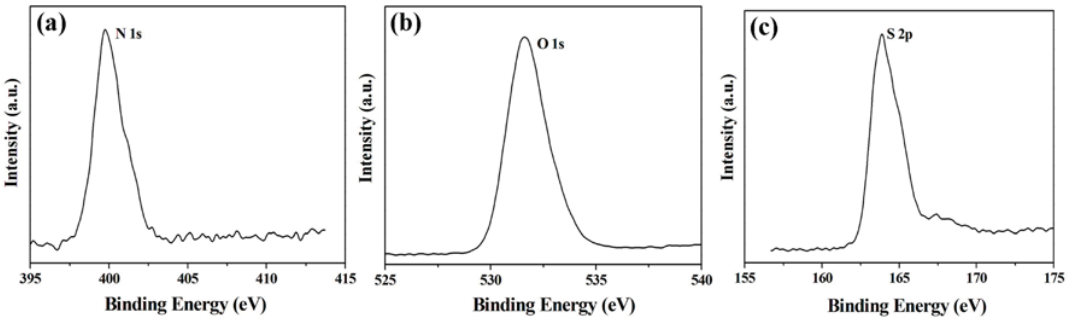

Fig. S2-XPS spectra of resultant CDs: (a) N 1s; (b) O 1s; (c) S 2p.

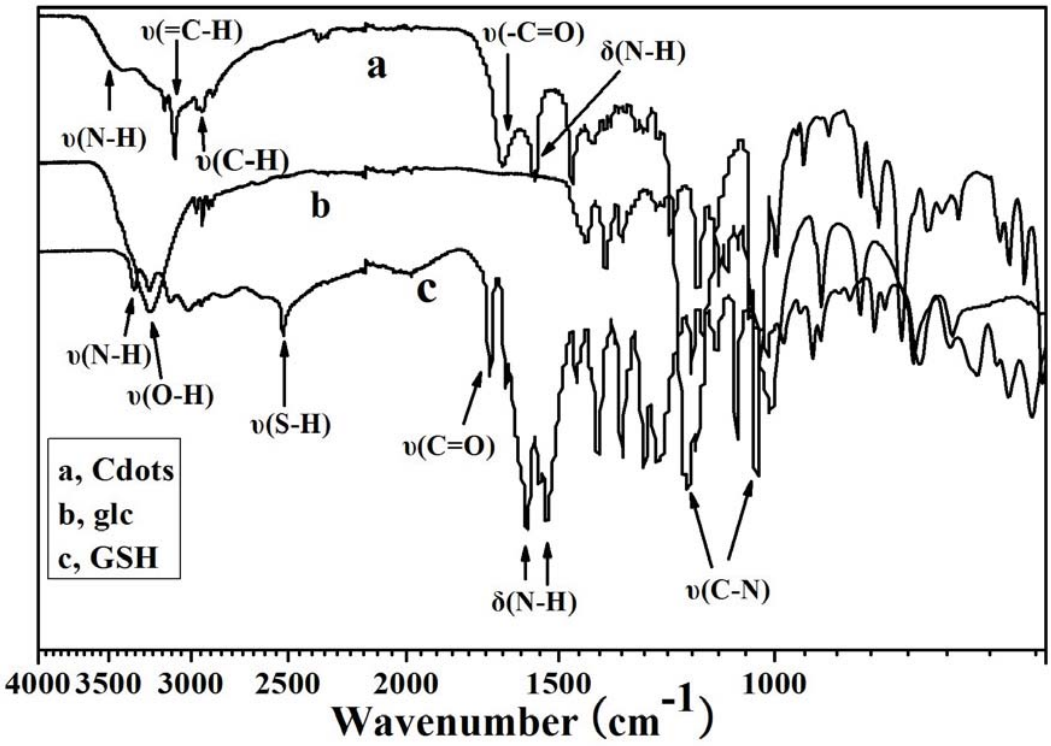

Fig. S3-The FT-IR spectra of (a) as-prepared CDs, (b) pure glc and (c) pure GSH

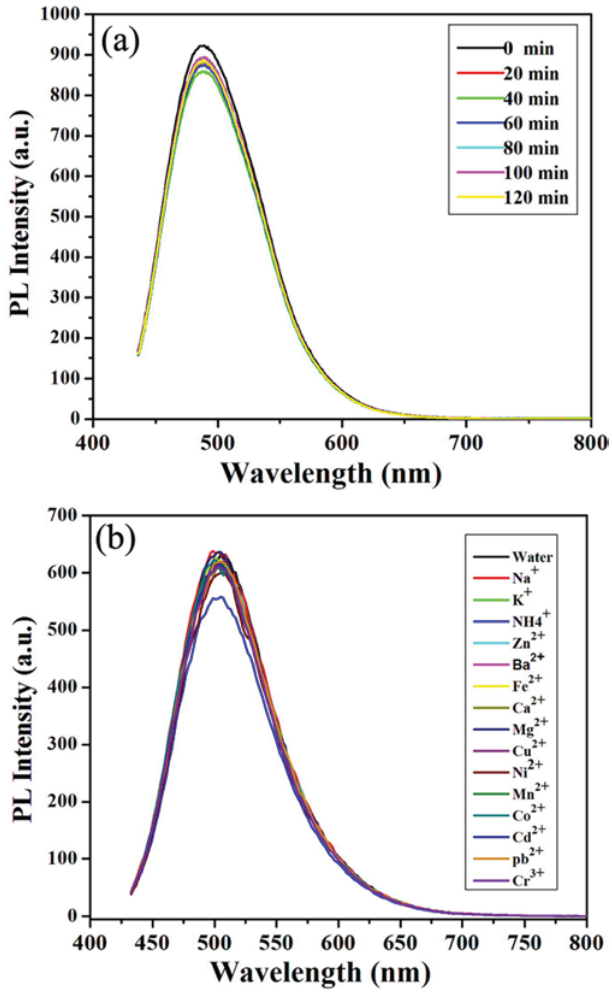

Fig. S4-The fluorescence spectra of CDs: (a) exposed under a 450 W xenon lamp for various time spans and (b) the presence of various metal ions

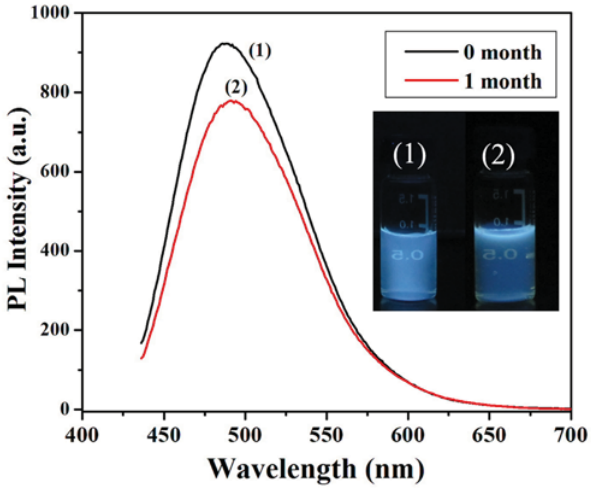

Fig. S5-The fluorescence spectra of (1) as-prepared CDs and (2) storing under normal condition for one months, inset display the photographs of fluorescent

CDs under 365 nm UV light illumination.

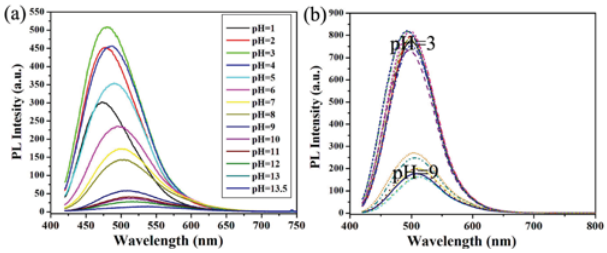

Fig. S6-(a) fluorescence spectra of CDs responses to pH ranging systematically from 1 to 13.5; (b) fluorescence spectra of CDs under pH=3 and pH=9

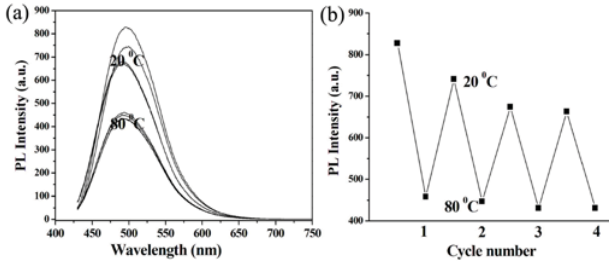

Fig. S7-(a) fluorescence spectra of CDs under 20 and 80 ºC; (b) PL intensity upon the cyclic switching of CDs under alternating conditions of 20 and 80 ºC.